

Electronic Supplementary Information (ESI):

**Rapid construction of 3D foam-like carbon nanoarchitectures *via* a simple
photochemical strategy for capacitive deionization**

*Haiyan Duan,[‡] Tingting Yan,[‡] Zhongxun An, Jianping Zhang, Liyi Shi and Dengsong Zhang**

Research Center of Nano Science and Technology, Shanghai University, Shanghai 200444, China.

**Tel: 86 21 66137152; E-mail: dszhang@shu.edu.cn*

‡ These authors contributed equally to this work.

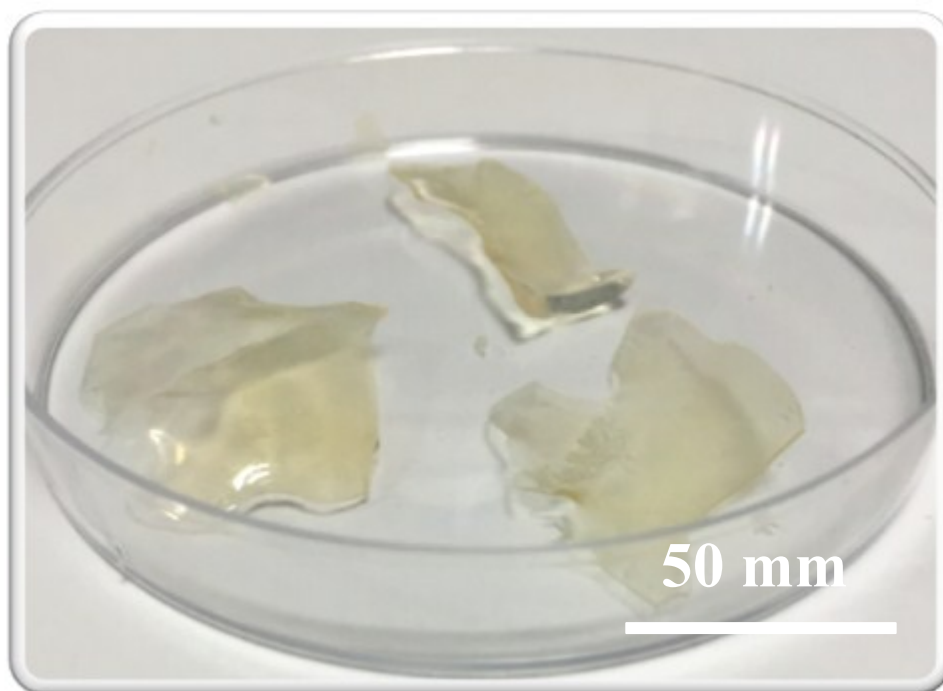


Fig. S1 Photograph of the UV-curable nanocomposites.

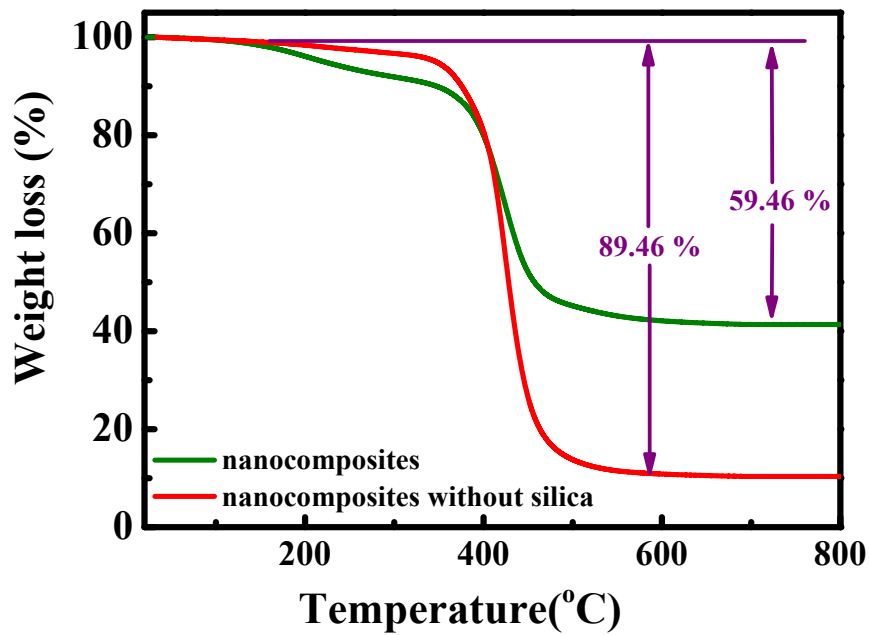


Fig. S2 Thermo-gravimetric curves of nanocomposites under an N₂ atmosphere with a heating rate of 10°C/min.

It can be seen that almost no weight loss can be observed beyond 600°C and they present the similar downward trends of nanocomposites and nanocomposites without SiO₂. And it shows a carbon conversion of approximately 11% at 600°C, elucidating that we obtained completely carbon by calcination at 900°C, which is in accordance with the XRD results. In addition, the difference value of weight loss between the nanocomposites and nanocomposites without SiO₂ can be attributed to the introduced SiO₂ with a mass percent of 30%.

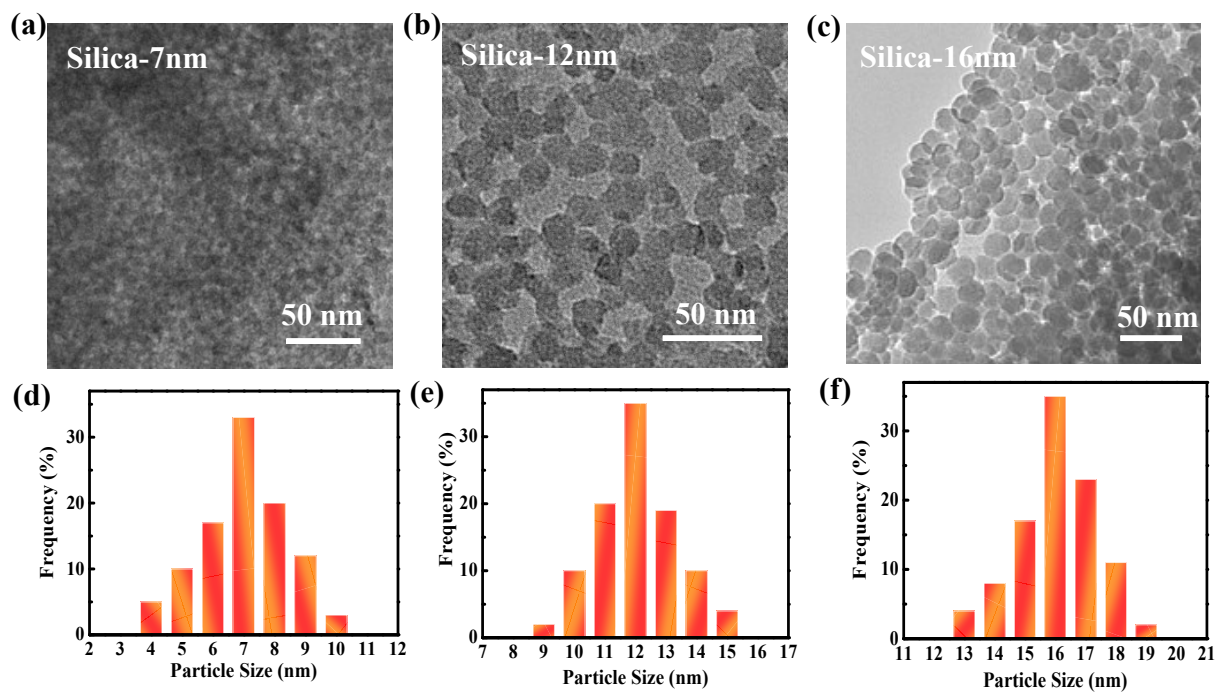


Fig. S3 TEM images and the corresponding particle size distribution histograms of silica with different pore size (a,b) 7nm, (c,d) 12nm and (e,f) 16nm.

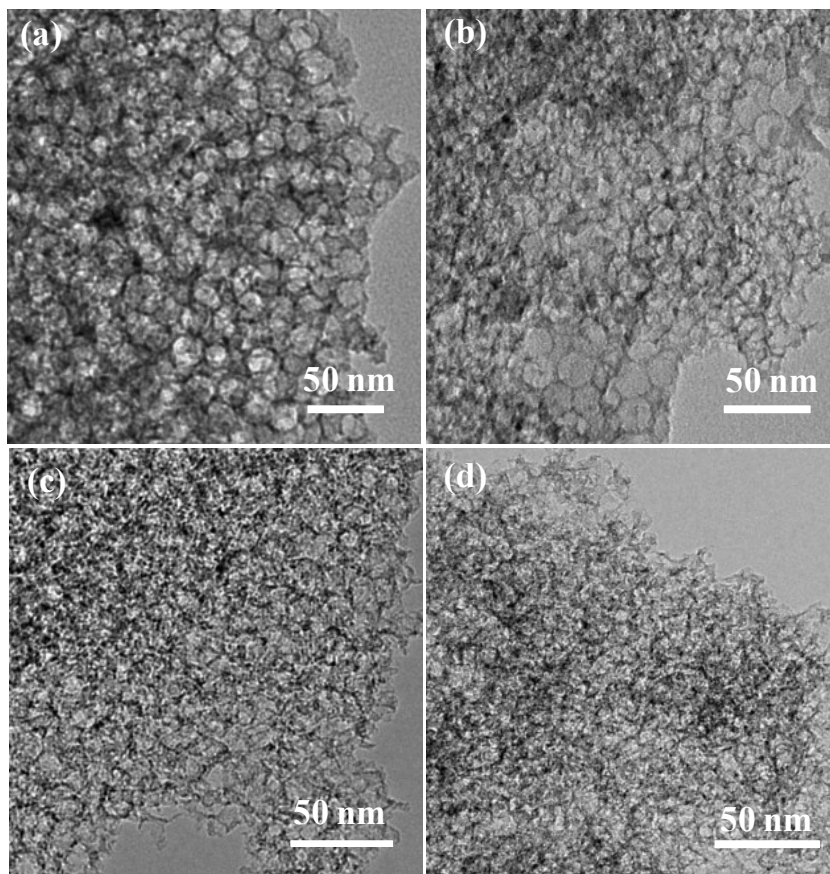


Fig. S4 TEM images of (a) 3DFCN-16-20, (b) 3DFCN-16-40, (c) 3DFCN-12-20 and (d) 3DFCN-12-40.

The morphology of the as-prepared 3DFCN with different silica mass percent were investigated as shown in Fig. S4. It can be seen that the wall thickness was tunable from 2 to 5 nm at a mass percent of 20 to 40 for 3DFCN-16, without influencing the homogeneous foam-like porous morphology. However, there are some structural damage and collapse for 3DFCN-16-40 due to an excess of silica. Similarly, the morphological structures of 3DFCN-12 maintain the uniform 3D foam-like mesoporous structures at a feed ratio of 20. However, 3DFCN-12-40 tends to form irreversible agglomerates or even restack, causing the broken of partial carbon structures, which is similar to that of 3DFCN-7-40.

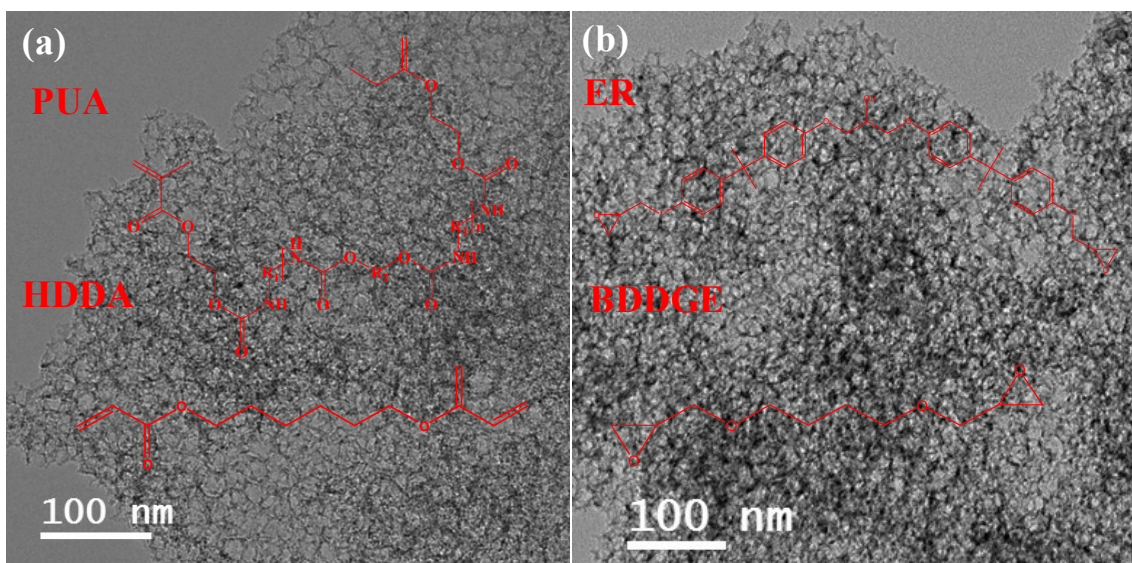


Fig. S5 TEM images of 3DFCN obtained by altering precursor: (a) 3DFCN-PUA/HDDA and (b) 3DFCN-ER/BDDGE.

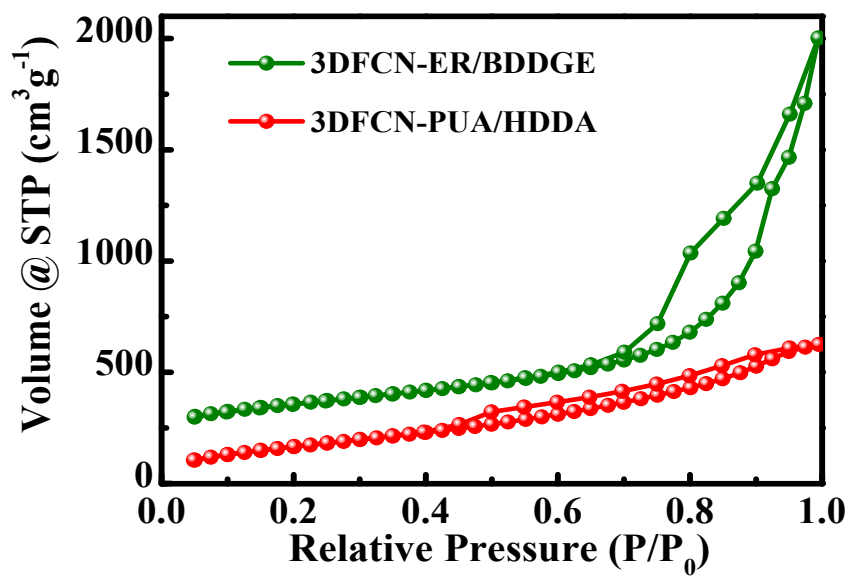


Fig. S6 N₂ adsorption–desorption isotherms of 3DFCN-PUA/HDDA and 3DFCN-ER/BDDGE.

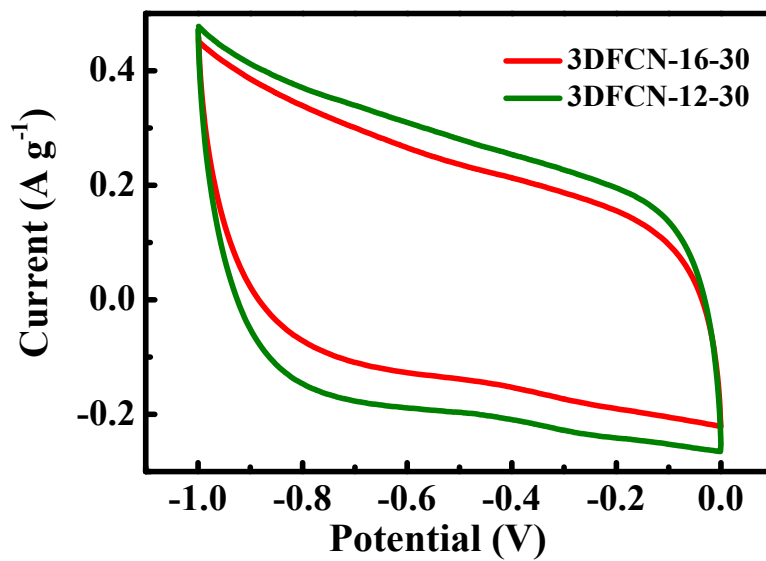


Fig. S7 CV curves of the 3DFCN at a scan rate of 1 mV s^{-1} . All the curves were obtained in a 0.5 M NaCl aqueous solution.

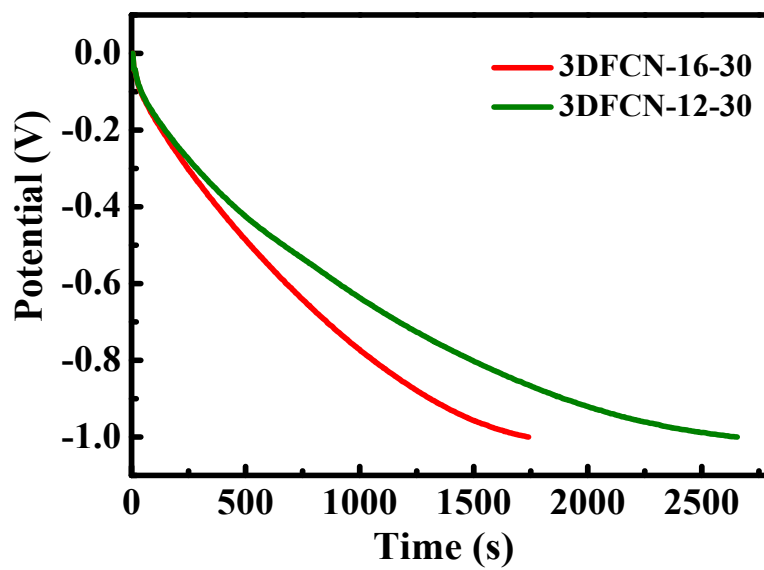


Fig. S8 GCD curves of 3DFCN at 0.2 A g^{-1} .

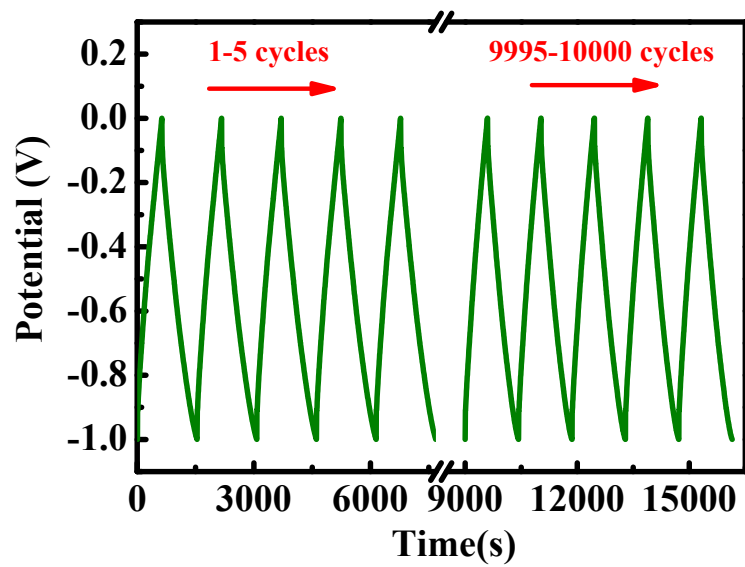


Fig. S9 Continuous GCD curves of the 3DFCN-7-30 electrode with a current density of 0.4 A g^{-1} . All the curves were obtained in a 0.5 M NaCl aqueous solution.

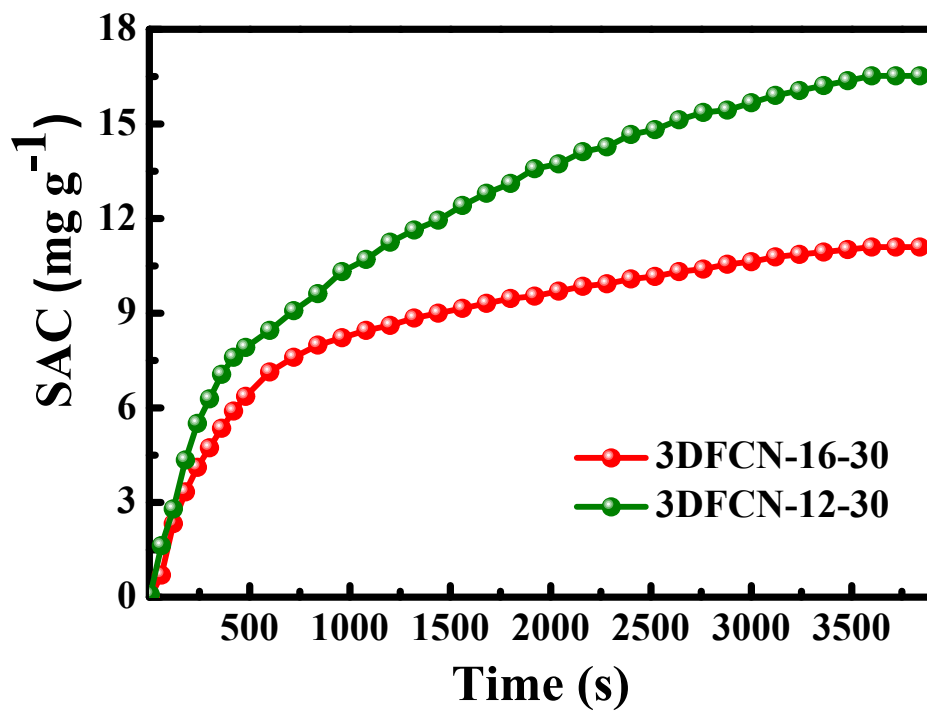


Fig. S10 Plots of SAC vs. time for 3DFCN in a 500 mg L^{-1} NaCl solution at 1.4 V.

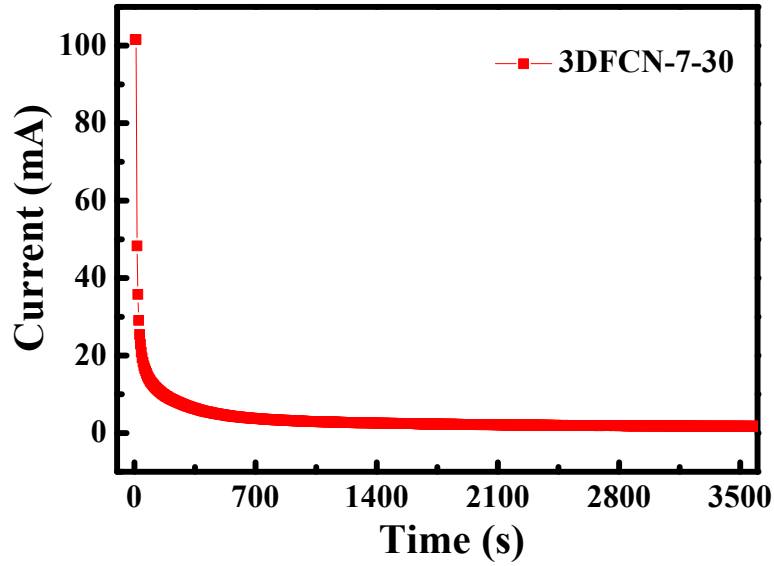


Fig. S11 The current transient for the 3DFCN-7-30 in a 500 mg L⁻¹ NaCl solution at 1.4 V.

Charge efficiency (λ) is a functional tool to gain insight into the double layer formed at the interface between the electrode and the solution, which reflects the ratio between the amounts of removed salt molecules and electrical charge,¹ which is obtained according to the following equation :

$$\lambda = \frac{\Gamma \times F}{\Sigma}$$

where F is the Faraday constant (96485 C mol⁻¹), Γ is the salt adsorption capacity (mol g⁻¹) and Σ (charge, C g⁻¹) is obtained by integrating the corresponding current.

To get a better understanding of the deionization behavior of the 3DFCN-7-30, the deionization experiments were carried out in 500 mg L⁻¹ feed concentration and a cell voltage of 1.4 V. The corresponding currents were monitored simultaneously. As calculated, the charge efficiency of the 3DFCN-7-30 is 0.54, and it keeps away from the theory value of 1.0. It is mainly caused by the following reasons: (i) the co-ion repulsion effect can account for the low charge efficiency.² (ii) the weak adhesion between the electrodes and current collector may lead to lower charge efficiency. (iii) the blocking effect of the binder could intensity the electric resistance of the electrodes and thus require more voltage consumption.

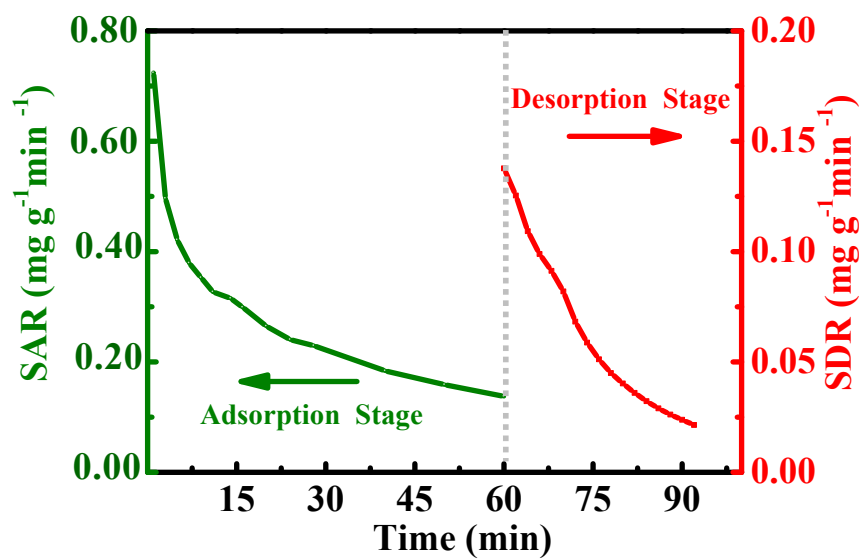


Fig. S12 Plots of SAR vs. time and salt desorption rate (SDR) vs. time for the 3DFCN-7-30 in a 100 mg L⁻¹

NaCl solution at 1.4 V.

Table S1 Comparison of SAC of various carbon electrode materials from the literature.

Electrode materials	Applied voltage [V]	Initial NaCl concentration [mg L ⁻¹]	SAC [mg g ⁻¹]	Ref.
Graphene	2.0	250	4.6	3
Mesoporous graphene	1.6	~500	15.2	4
Nitrogen doped carbon aerogel	1.5	~1463	8.2	5
N-PHCS ^a	1.4	500	13	6
Porous graphene	1.6	500	15	7
CFC-SRGO ^b	1.4	250	~8.07	8
Porous carbon spheres	1.4	50	~2.73	9
Porous carbon spheres	1.6	500	5.81	9
Carbon nanotubes	1.2	1000	3.78	10
Carbon fibre cloths	1.4	250	~5.27	8
3D graphene	1.4	300	2.17	11
Carbon nanofiber networks	1.2	1000	12.8	10
Activated mesoporous carbon sheets	1.4	1000	3.5	12
3D porous graphene	1.4	300	8.97	11
3D graphene	1.4	500	9.48	13
3DFCN-7-30	1.4	1000	20.9	This work
3DFCN-7-30	1.4	500	17.5	This work

^a Nitrogen-doped porous hollow carbon spheres

^b Carbon fibre cloth (CFC) and sulphonated reduced graphene oxide (SRGO) composites

References

- 1 T. Kim, J.E. Dykstra, S. Porada, d.W.A. Van, J. Yoon and P.M. Biesheuvel, *J. Colloid. Interf. Sci*, 2015, **446**, 317-326.
- 2 H. Lei, T. Yan, H. Wang, L. Shi, J. Zhang and D. Zhang, *J. Mater. Chem. A*, 2015, **3**, 5934-5941.
- 3 B. Jia and L. Zou, *Chem. Phys. Lett*, 2012, **548**, 23-28.
- 4 X. Gu, M. Hu, Z. Du, J. Huang and C. Wang, *Electrochim. Acta*, 2015, **182**, 183-191.
- 5 G. Rasines, P. Lavela, C. Macías, M.C. Zafra, J.L. Tirado, J.B. Parra and C.O. Ania, *Carbon*, 2015, **83**, 262-274.
- 6 S. Zhao, T. Yan, H. Wang, G. Chen, L. Huang, J. Zhang, L. Shi and D. Zhang, *Appl. Surf. Sci*, 2016, **369**, 460-469.
- 7 W. Shi, H. Li, X. Cao, Z.Y. Leong, J. Zhang, T. Chen, H. Zhang and H.Y. Yang, *Sci. Rep*, 2016, **6**, 18966-18975.
- 8 H. Li, F. Zaviska, S. Liang, J. Li, L. He and H.Y. Yang, *J. Mater. Chem. A*, 2014, **2**, 3484-3491.
- 9 Y. Liu, L.K. Pan, T.Q. Chen, X.T. Xu, T. Lu, Z. Sun and D.H.C. Chua, *Electrochim. Acta*, 2015, **151**, 489-496.
- 10 Y. Liu, T. Lu, Z. Sun, D.H.C. Chua and L.K. Pan, *J. Mater. Chem. A*, 2015, **3**, 8693-8700.
- 11 A.G. El-Deen, R.M. Boom, H.Y. Kim, H. Duan, M.B. Chan-Park and J.-H. Choi, *ACS Appl. Mater. Interfaces*, 2016, **8**, 25313-25325.
- 12 C. Tsouris, R. Mayes, J. Kiggans, K. Sharma, S. Yiacoumi, D. DePaoli and S. Dai, *Environ. Sci. Technol*, 2011, **45**, 10243-10249.
- 13 P. Liu, H. Wang, T. Yan, J. Zhang, L. Shi and D. Zhang, *J. Mater. Chem. A*, 2016, **4**, 5303-5313.